Gas-phase synthesis and characterization of heteroleptic divalent germanium compounds by FVT/UV-PES

Anna Chrostowska [a],*, Virginie Lemierre [a], Alain Dargelos [a], Patrick Baylère [a], William J. Leigh [b], Ghassoub Rima [c], Lothar Weber [d], Michaela Schimmel [d]

[a] Institut Pluridisciplinaire de Recherche sur l'Environnement et les Matériaux, UMR 5254, Université de Pau, Hélioparc Pau-Pyrénées – 2, Av. P. Angot, 64053 Pau Cedex 9, France
[b] Department of Chemistry, McMaster University, 1280 Main Street West, Hamilton, Ontario, Canada L8S 4M1
[c] Hétérochimie Fondamentale et Appliquée, UMR 5069, Université Paul Sabatier, 118, route de Narbonne, 31062 Toulouse Cedex 4, France
[d] Fakultät für Chemische, Universität Bielefeld, D-33615 Bielefeld, Germany

ABSTRACT

The flash vacuum thermolysis/UV photoelectron spectroscopic (FVT/UV-PES) technique has been applied for the synthesis of three cyclic germanediyls containing oxo-thio, oxo-amino, and thio-amino substitution at germanium. The three compounds (**4b**, **5b** and **6b**) were prepared from the corresponding 3,4-dimethyl-1-germacyclopent-3-enes (**4a**, **5a** and **6a**) by thermal cheletropic elimination, and the photoelectron spectra of both sets of molecules were measured. The course of the thermolysis reactions has also been confirmed by mass spectrometric methods and the results of chemical trapping experiments. The assignment of the PE spectral bands for the two series of molecules has been carried out with the aid of time dependent DFT (TD-DFT) and outer valence green's function (OVGF) calculations. The results indicate that the strong σ-withdrawing effect of oxygen and the strong π-donating effect of nitrogen are the two main factors affecting the electronic structures of these germylene derivatives.

© 2008 Elsevier B.V. All rights reserved.

1. Introduction

The chemistry of germylenes, the germanium analogues of carbenes, has been extensively investigated over the last 30 years [1]. One general class of these compounds that continues to be of particular interest is α,α′-heteroatom-substituted germylenes [2]. These species are stabilized thermodynamically by π-electron donation into the empty 4p-orbital of the divalent germanium atom, but generally must contain bulky or coordinating ligands in order to gain the kinetic stabilization that is required to prevent polymerisation or oligomerization reactions, and hence permit their isolation.

The first isolable diaminogermylenes :Ge(NRSiMe$_3$)$_2$ (R=SiMe$_3$, t-Bu) were synthesized by Harris and Lappert in 1974 [3] and later characterized by photoelectron spectroscopy [4]. However, the most significant advances in this field began with the synthesis and isolation by Herrmann and co-workers of the formally aromatic germylene 1,3-di-*tert*-butyl-1,3,2-diazagermol-2-ylidene [5], analogous to the well-known stable carbene of Arduengo and co-workers [6]. The electronic structures and bonding in these and the corresponding silicon compound [7] have been studied by photoelectron [8] and core shell excitation [9] spectroscopies and by theoretical methods [10,11], and are reasonably well understood. These studies show quite clearly that the high thermodynamic stabilities of these compounds are due to strong pπ–pπ delocalisation involving both the nitrogen lone pairs and the C=C bond, but are dominated by the interactions with nitrogen. The highest occupied molecular orbital (HOMO) in both the germylene and silylene is a π-type MO corresponding to in-phase mixing of the nitrogen lone pairs and the 4p- or 3p-orbitals on the metallylene center, mixed (out-of-phase) with the C=C π-orbital; the latter contributes less in the HOMO of the germylene than in that of the silylene. The σ lone pair orbital is responsible for the second ionization band. Indeed, theoretical calculations indicate a similar electronic structure and ordering of the two highest MOs in the C–C saturated 1,3,2-diazagermolin-2-ylidenes [10]. This has been verified recently in our laboratories, in the photoelectron spectrum of the (transient) 1,3,2-diazagermolin-2-ylidene derivative 1b, prepared by FVT of 1a (Eq. (1)) [12]. The molecule lacks the steric bulk about germanium that is required for long-term stability [5], but

* Corresponding author.
E-mail addresses: anna.chrostowska@univ-pau.fr (A. Chrostowska), leigh@mcmaster.ca (W.J. Leigh).

can nevertheless be detected and characterized in the gas phase over a limited temperature range.


1a   **1b**   DMB   (1)
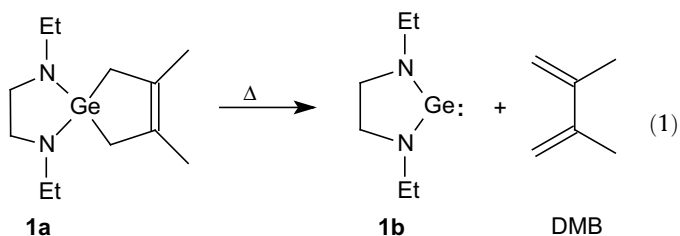
α-Oxo- and α-thio-substituted germylene derivatives have also been studied. Alkoxy- and aryloxygermylenes generally exist in associated oligomeric form in the liquid state [13], in the absence of sterically bulky [14,15] or internally-coordinating [16,17] substituents. Jutzi and Steiner have successfully prepared a series of dithiogermylenes :Ge(SR)$_2$ [18], but found these species to exist only in associated dimeric or trimeric forms. This is also the case with the (cyclic) dithio- and oxathiolanegermanediyls developed by Satgé and Maziéres and their co-workers [19].

Recently, the direct measurement of the UV photoelectron spectra of the cyclic dioxo- and dithiogermylenes **2b** and **3b**, generated in monomeric form by FVT of the corresponding 3,4-dimethyl-1-germacyclopent-3-ene derivatives **2a** and **3a**, respectively (Eq. (2)) [20] has been carried out in the Pau laboratories, using a similar methodology as that employed in our earlier study of **1a** [12]. As in the latter compound, the presence of the α,α′-heteroatoms induces significant thermodynamic stabilization as a result of delocalisation of the π lone pairs associated with the α,α′-heteroatoms into the unoccupied 4p-orbital of the germanium atom.

2a (X = O)   **2b**   (2)
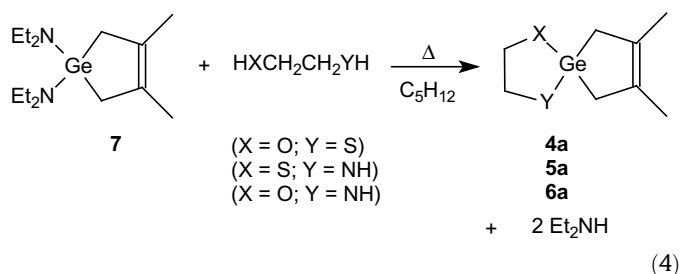**3a** (X = S)   **3b**   DMB
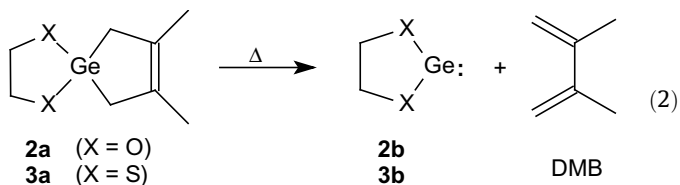
In the present paper, we focus our attention on the heteroleptic O, N and S α,α′-disubstituted germanediyls **4b–6b** (Eq. (3)), in order to probe the effects of dissymmetric substitution on electronic structure and bonding in α,α′-heteroatom-substituted germylenes. Despite the anticipation of rather lower hydrolytic stabilities of the amino-substituted derivatives (**5a** and **6a**) owing to the absence of stabilizing alkyl substituents at nitrogen [21], we were encouraged to attempt their synthesis by the promise of a series of heteroleptic germylene derivatives with the simplest possible set of heteroatom substituents at germanium. As in our previous studies, flash vacuum thermolysis techniques have been employed for the generation of these short-lived species under conditions where their UV photoelectron spectra can be measured, and the spectra have been analysed with the aid of time dependent density functional theory (B3LYP/6-311G(d,p)) and outer valence green's function (6-311G(d,p)) calculations. As we have discussed previously [22], and shown specifically in previous studies of transient germylenes by PES [12,20,23], these methods offer a quite reasonable compromise between the quality of the results and the cost associated with calculations of this type. The course of the thermolysis reactions has also been verified by mass spectrometric methods and the results of chemical trapping experiments.

4a (X = O; Y = S)   **4b**   (3)
5a (X = S; Y = NH)   **5b**   DMB
**6a** (X = O; Y = NH)   **6b**
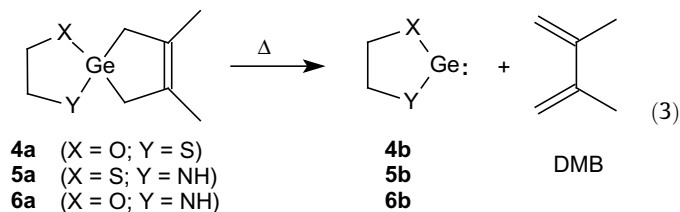
2. Results and discussion

The germylene precursors **4a–6a** were prepared by condensation of 2-thioethanol, 2-aminoethanethiol, and 2-aminoethanol, respectively, with 1,1-diethylamino-1-germa-3,4-dimethylcyclopent-3-ene (7; Eq. (4)); **4a** has been reported previously [24]. Compounds **5a** and **6a** were isolated by vacuum distillation as air- and moisture-sensitive liquids. According to the ^{1}H and ^{13}C NMR spectra **5a** is part (40%) of a mixture of products due to partial decomposition, of which only 2-aminoethanethiol could be identified. Despite several attempts, we were unable to obtain either compound in pure form. Nevertheless, the EI mass spectra of the compounds, recorded by gentle distillation directly in the inlet probe of the mass spectrometer, were fully consistent with their proposed structures (see Section 4)

7   (X = O; Y = S)   **4a**
                 (X = S; Y = NH)   **5a**
                 (X = O; Y = NH)   **6a**

                                          + 2 Et$_2$NH

                                                                                        (4)

The course of the FVT of the three compounds was examined by mass spectrometry, by rapid heating of the distilled materials within the inlet probe of the spectrometer and comparing the resulting mass spectrum of the thermolysed sample to that recorded without heating. For example, the mass spectrum of **4a** exhibits ions located at m/z = 232 (66, [M]$^+$) and 150 (30, [M−DMB]$^+$), 149 (38, [M−(DMB+H)]$^+$), and 82 (72, [DMB]$^+$) in relative intensities of (2.20):(1):(1.20):(2.30). Flash thermolysis of the sample resulted in a decrease in the intensity of the 232 amu ion and increases in those of the 150, 149, and 82 amu ions, resulting in an intensity ratio of (0.60):(1):(1.40):(13.60). Analogous changes occur in the spectra of **5a** and **6a** upon thermolysis at similar temperatures. These results are consistent with [4+1] cheletropic cycloreversion to liberate 2,3-dimethyl-1,3-butadiene (DMB) and the corresponding germylenes **4b–6b**, upon FVT of **4a–6a**.

Additional support for the course of the thermolyses of **4a–6a** was obtained from chemical trapping experiments using dimethyldisulfide as a germylene trap, thermolysing the compounds at 120 °C in the neat disulfide as solvent and analyzing the products of the reactions by mass spectrometry. In each case, the mass spectrum of the product mixture exhibited prominent molecular ions corresponding to the expected S–S insertion product of the germylene and the disulfide (**4c–6c**), along with (tetramethylthio)germane [25], which is presumably formed by secondary thermolytic reactions of the primary trapping products (Eq. (5))

4a (X = O; Y = S) **4c**
5a (X = S; Y = NH) **5c** + DMB + Ge(SMe)$_4$
6a (X = O; Y = NH) **6c**

(5)
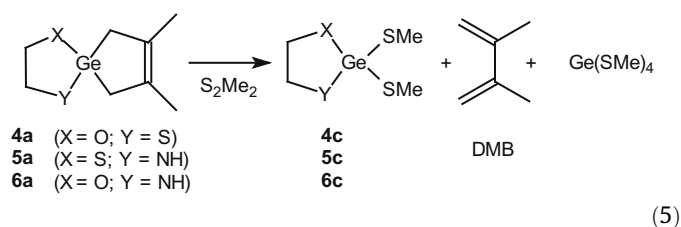
2.1. UV photoelectron spectra of germacyclopentenes **4a**–**6a**

Representative UV photoelectron spectra of the three germacyclopentene derivatives (**4a**–**6a**) are shown in Figs. 1–3. The spectrum of the oxa–thia compound (**4a**; Fig. 1) exhibits a sharp first band containing easily discernible features at 8.6 and 8.7 eV, followed by three well-resolved bands at 9.45, 10.3 and 10.9 eV. That of the aza–thia compound (**5a**; Fig. 2) shows two bands, the first containing three features at 8.35, 8.55 and 8.7 eV, and the second with two maxima at 10.0 and 10.2 ev. Finally, the spectrum of the oxa–aza compound (**6a**; Fig. 3) displays three main ionizations centred at 8.5, 9.3 and 10.6 eV, and a weakly discernible feature at 8.7 eV.

Theoretical calculations were carried out on **4a**–**6a** in order to assist in the assignment of the PE spectra of these compounds. Geometry optimizations were carried out at the B3LYP/6-311G(d,p) level of theory, the results of which are listed in Table 1. The calculated Ge-heteroatom bond distances are in each case close to (but slightly longer than) the standard Ge–O, Ge–S, and Ge–N bond lengths in four-coordinate germanium compounds of 1.760 Å, 2.230 Å, and 1.850 Å, respectively [26], and the Ge–O and Ge–S bond distances are slightly longer in the nitrogen-containing derivatives (**6a** and **5a**) compared to their values in **4a**. In each case, the germacyclopentene ring is planar and the heteroatom-containing ring is twisted, with twist angles of 24.9°, 24.0°, 22.2° in **4a**, **5a**, and **6a**, respectively. The sum of the bond angles about nitrogen in **5a** and **6a** is very close to the value expected for sp^3-hybridization at this center (ΣN = 329.8°) [26]. Finally, we note that the aza–thia derivative (**5a**) exhibits the largest X–Ge–Y bond angle and the aza–oxa derivative (**6a**) the smallest, distinguishing the latter compound as the one exhibiting the shortest distance between the two heteroatoms.
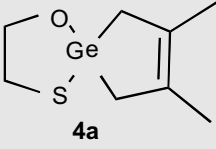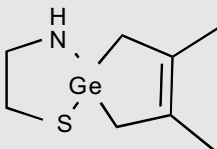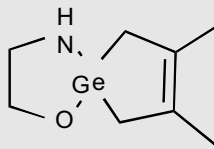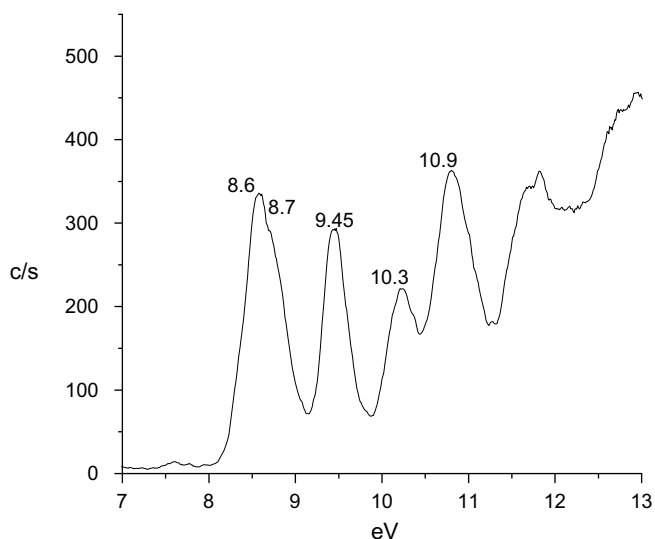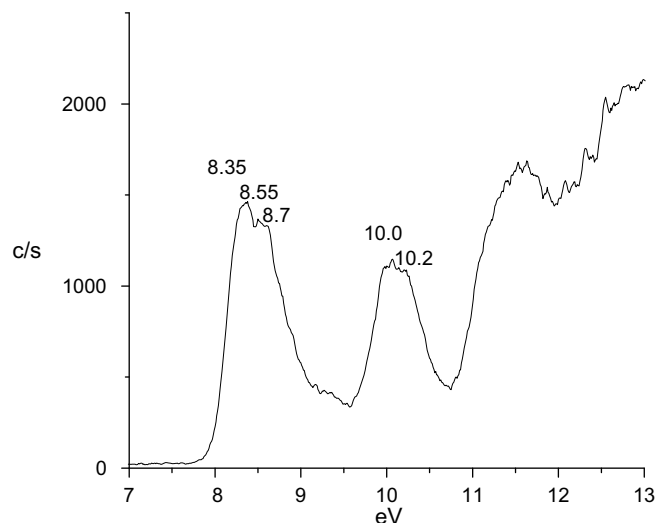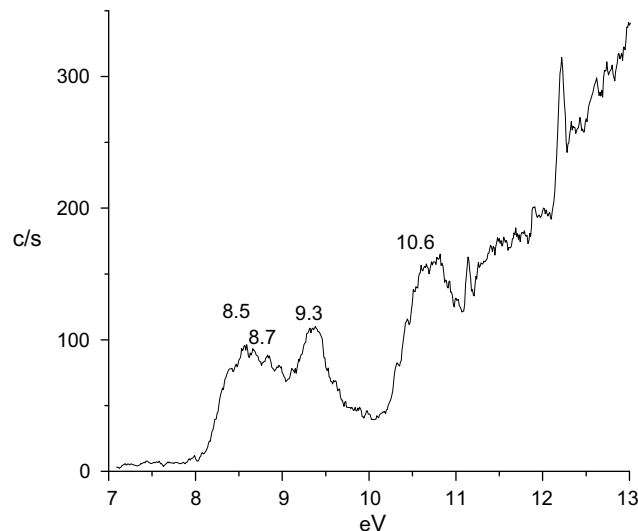

Fig. 2. Photoelectron spectrum of **5a**.

Fig. 3. Photoelectron spectrum of **6a**.

Ionization energies for **4a**, **5a** and **6a** were calculated by three methods: TD-DFT, OVGF, and empirical correction of the calculated Kohn–Sham energies, as employed in our previous studies of GeH$_2$, GeMe$_2$, GePh$_2$, and the germacyclopentene derivatives from which they were generated [23]. The calculated IEs and corresponding MO-assignments for the three compounds are listed in Tables 2–4. The HOMOs in **4a** and **5a** are in both cases localized at the sulfur lone pair, mixed with the antibonding combination of the σ_{Ge-C} bonds (σ_{Ge-C}^-) of the same symmetry, while that in **6a** is localized at the nitrogen lone pair, mixed in a similar way with the σ_{Ge-C} bonds. The second-highest MOs in all three molecules are the $\pi_{C=C}$ MOs, while the third-highest are strongly localized on the oxygen (**4a** and **6a**) or nitrogen (**5a**) lone pair MOs.

The data listed in Tables 2–4 show that in all three cases, the OVGF method reproduces the positions of the five lowest energy ionization bands considerably more successfully than the TD-DFT method. The differences are particularly large in the case of **4a**, where ΔSCF (TD-DFT) overestimates the first ionization energy (associated with the π-type MO localized mainly on sulfur) by 0.49 eV, while the OVGF method underestimates it by only 0.17 eV. The same magnitude of variation is observed in the second

Fig. 1. Photoelectron spectrum of **4a**.

Table 1
Calculated (B3LYP/6-311G(d,p)) geometrical parameters (distances in Å, bond angles in °) of **4a**, **5a** and **6a**.

	4a	5a	6a
Ge–S	2.255	2.271	–
Ge–N	–	1.870	1.865
Ge–O	1.815	–	1.822
X–Y	3.010	3.076	2.682
X–Ge–Y	94.7	95.4	93.3
C–Ge–C	93.4	92.9	93.4
Twist angle	24.9	24.0	22.2
ΣN	–	332.6	329.8

IE, which is associated with the $\pi_{C=C}$ orbital, while closer agreement between the two methods (TD-DFT, OVGF) is noted for the third IE, the π-type MO localized mainly on oxygen. There appears to be no consistent trend in the TD-DFT IEs for the three compounds, making it difficult to pinpoint the precise reasons for the poor performance of the method relative to the OVGF method in reproducing the experimental IEs. As can be seen from Tables 2–4, TD-DFT consistently overestimates the four lowest IEs in the case of **4a**, consistently underestimates them in the case of **5a**,

Table 2
Calculated (6-311G(d,p)) ionization energies for **4a** (all values in eV).

Exp.	MO type	$-\varepsilon_i^{KS}$	TD-DFT	OVGF	"Corrected" $x = 2.00$[b]
8.6	$n_S^\pi - \sigma_{Ge-C}^-$	6.40	9.09[a]	8.43	8.60
8.7	$\pi_{C=C}$	6.49	9.26	8.54	8.69
9.45	$n_O^\pi - \sigma_{Ge-C}^-$	7.15	9.66	9.54	9.35
10.3	$(\sigma_{Ge-S} + n_S^\sigma) - n_O^\sigma$	8.02	10.67	10.10	10.22
10.9	$n_O^\sigma + \sigma_{Ge-O}$	8.42	10.88	11.00	10.62

[a] ΔSCF value.
[b] Empirical energy correction (see Section 4.7).

Table 3
Calculated (6-311G(d,p)) ionization energies for **5a** (all values in eV).

Exp.	MO type	$-\varepsilon_i^{KS}$	TD-DFT	OVGF	"Corrected" $x = 2.17$[b]
8.35	$n_S^\pi - \sigma_{Ge-C}^-$	6.18	7.97[a]	8.21	8.35
8.55	$\pi_{C=C}$	6.40	8.06	8.45	8.57
8.7	$n_N^\pi - \sigma_{Ge-C}^-$	6.54	8.15	8.77	8.71
10.0	$\sigma_{Ge-S} + n_S^\sigma$	7.87	9.63	9.91	10.04
10.2	σ_{Ge-C}^-	8.05	9.75	10.19	10.22

[a] ΔSCF value.
[b] Empirical energy correction (see Section 4.7).

Table 4
Calculated (6-311G(d,p)) ionization energies for **6a** (all values in eV).

Exp.	MO type	$-\varepsilon_i^{KS}$	TD-DFT	OVGF	"Corrected" $x = 2.11$[b]
8.5	$n_N^\pi - \sigma_{Ge-C}^-$	6.39	8.81[a]	8.46	8.50
8.7	$\pi_{C=C}$	6.40	8.95	8.72	8.51
9.3	$n_O^\pi - \sigma_{Ge-C}^-$	6.79	9.08	9.25	8.9
10.6	$\sigma_{Ge-O} + n_O^\sigma$	8.04	10.27	10.70	10.15
	σ_{Ge-C}^-	8.25	10.64	10.84	10.36

[a] ΔSCF value.
[b] Empirical energy correction (see Section 4.7).

and over- or underestimates them in the case of **6a**. On the other hand, very few serious differences arise between the experimental IEs and those calculated using the OVGF method. The agreement with experiment is generally consistently better for the second through fifth IEs estimated from the Kohn–Sham "corrected" IE-values.

The second IEs, which are associated with the $\pi_{C=C}$ orbitals, vary slightly in the three compounds (**4a**, 8.7 eV; **5a**, 8.55 eV; **6a**, 8.7 eV). This sensitivity to substitution at germanium has been noted as well in the 3,4-dimethyl-1-germacyclopent-3-ene derivatives that have been studied previously [23]. Finally, there exists a global lowering of the entire set of IEs throughout the series **4a** > **6a** > **5a**. This can be explained as being due to the decreasing electronegativity of the three heteroatoms O > N > S, which directly influences the relative energies of the π lone pair orbitals ($n_S^\pi < n_N^\pi < n_O^\pi$).

For the series of germacyclopentenes **4a–6a**, the calculated IEs obtained with the OVGF and "correction" methods are thus in good general agreement with the experimental spectra. Less satisfactory correlations are obtained from the TD-DFT method, as was also found previously for hydrido-, methyl- and phenyl-substituted 3,4-dimethyl-1-germacyclopent-3-ene derivatives [23]. Since the calculated IEs associated with the lower-lying orbitals in the TD-
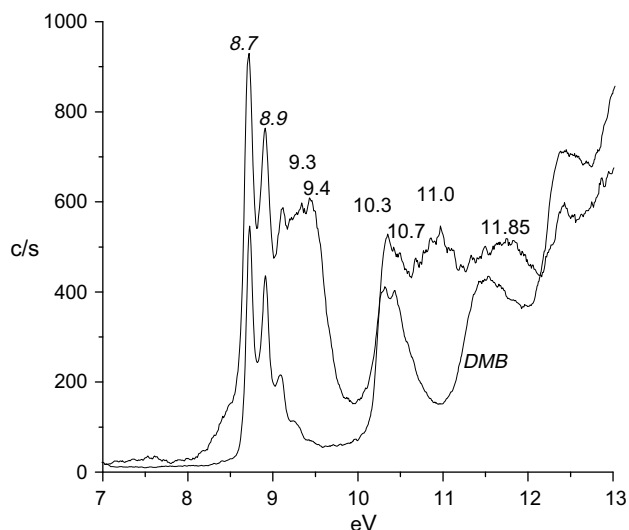
Fig. 4. Photoelectron spectra of **4a** thermolysed at 365 °C and of DMB.

DFT method depend directly on the calculated (ΔSCF) energy of the first ionic state relative to the ground state, the degree of accuracy with which the energies of these two states is determined is a crucial factor. As might thus be expected, calculations of the first ionic state energies at the HF/MP2/6-311G(d,p) level of theory for **4a–6a** reproduce the first experimental IEs much more closely (ΔSCF = 8.56 eV, 8.31 eV, and 8.70 eV for **4a**, **5a**, and **6a**, respectively) than the less expensive TD-DFT method.

2.2. FVT-PES of *4a–6a*: UV photoelectron spectra of germylenes *4b–6b*

The PE spectrum of **4a** exhibits noticeable changes at a thermolysis temperature of 365 °C (Fig. 4), where the characteristic ionization bands due to DMB at 8.7, 8.9, 9.1 and 10.3 eV have appeared, the 8.6–8.7 eV bands due to the precursor have disappeared, and two new broad ionization bands spanning 9.15–9.45 and 10.5–11.4 eV have appeared in the spectrum. The first of these new bands exhibits features centered at 9.3 and 9.4 eV, while the second exhibits features at 10.7, 11.0, and 11.85 eV. Only bands assignable to DMB and 2-thioethanol could be discerned in spectra recorded at higher thermolysis temperatures.

The spectrum of **5a** exhibits changes at 380 °C, again showing the appearance of the characteristic bands due to DMB at 8.7, 8.9 and 9.1 eV, and new ionization bands centered at 8.4, 9.3 and 9.9 eV (Fig. 5).

The aza–oxa derivative **6a** proved to be much more difficult to sort out than the others. Spectra recorded at thermolysis temperatures up to *ca.* 205 °C exhibited ionizations due only to **6a**, while those recorded above 260 °C showed mainly ionizations due to DMB and weak ionizations due to 2-aminoethanol [27]. The spectrum recorded at 240 °C (see Fig. 6) exhibits the three bands characteristic of DMB at 8.7, 8.9 and 9.1 eV, in addition to three new bands at 8.8, 9.45 (as a high energy shoulder on the 9.3 eV band due to the precursor) and 10.5 eV.

It is important to emphasize that in all three cases, the thermolysis reaction is evidenced by the appearance of the IEs due to DMB. Thermolysis temperatures higher than those indicated above appeared to result in total decomposition of the samples, as the only IEs that could be clearly distinguished were those due to DMB and HXCH$_2$CH$_2$YH. It is thus evident that the corresponding germylenes are themselves prone to thermal decomposition, as they can be detected only over a narrow temperature range in each case. We did
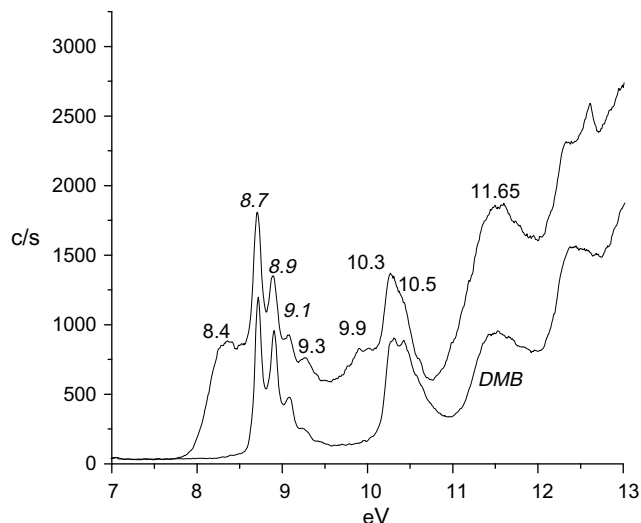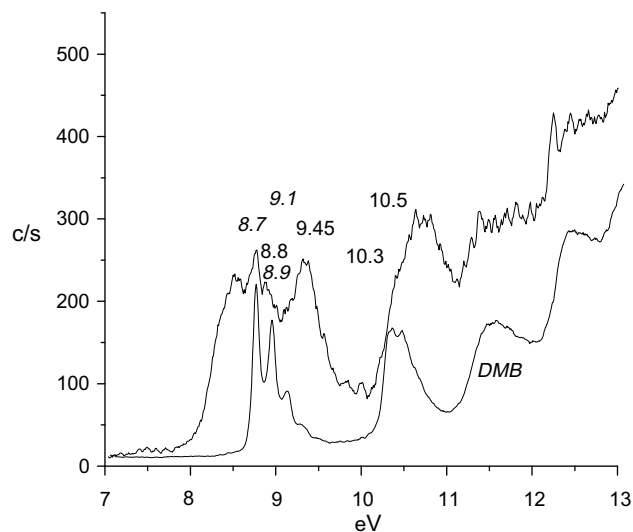

Fig. 6. Photoelectron spectra of **6a** thermolysed at 240 °C and of DMB.

Table 5
Calculated (B3LYP/6-311G(d,p)) geometrical parameters (distances in Å, bond angles in °) of **4b**, **5b** and **6b**.

	4b	5b	6b
Ge–S	2.282	2.288	–
Ge–N	–	1.843	1.843
Ge–O	1.813	–	1.828
X–Y	2.939	2.904	2.533
X–Ge–Y	91.0	88.7	87.3
Twist angle	22.4	22.5	19.8
ΣN	–	357.9	357.7

not investigate the course or mechanism of the decomposition process further [5].

Geometry optimizations for germylenes **4b–6b** were also carried out at the B3LYP/6-311G(d,p) level of theory, and the results are listed in Table 5. We note a shortening of the germanium–nitrogen bond distances, a lengthening of the germanium–sulfur distances, and nearly unchanged germanium–oxygen bond lengths in the germylenes compared to the corresponding bonds in the precursors. The calculated Ge–N bond distances in **5b** and **6b** are in good agreement with experimental values (Ge–N = 1.833 Å) reported for saturated cyclic diaminogermylenes [7]. Whereas the sums of the calculated bond angles about nitrogen in **5a** and **6a**

Table 6
Calculated (6-311G(d,p)) ionization energies for **4b** (all values in eV).

Exp.	MO type	$-\varepsilon_i^{KS}$	TD-DFT	OVGF	"Corrected" x = 2.46[b]
9.3	$n_S^\pi - n_O^\pi$	6.84	9.06[a]	9.06	9.3
9.4	$n_{Ge} - n_S^\sigma$	7.11	9.32	9.14	9.57
10.7	$n_S^\pi + n_O^\pi$	8.36	10.46	11.18	10.82
11.0	$n_S^\sigma - n_O^\sigma$	8.45	10.54	11.20	10.91
11.85	σ_{Ge-S}	9.34	11.55	11.52	11.80

[a] ΔSCF value.
[b] Empirical energy correction (see Section 4.7).

Fig. 5. Photoelectron spectra of **5a** thermolysed at 380 °C and of DMB.

Table 7
Calculated (6-311G(d,p)) ionization energies for **5b** (all values in eV).

Exp.	MO type	$-\varepsilon_i^{KS}$	TD-DFT	OVGF	"Corrected" $x = 2.12$[b]
8.4	$n_S^\pi - n_N^\pi$	6.28	8.38[a]	8.49	8.4
9.3	$n_{Ge} - n_S^\sigma$	6.81	8.90	8.76	8.93
9.9	$n_S^\pi - n_N^\pi$	7.47	9.74	9.77	9.59
10.5	$n_S^\sigma - \sigma_{Ge-N}$	8.57	10.78	10.80	10.69
11.65	$\sigma_{Ge-S} - \sigma_{Ge-N}$	9.52	11.61	11.88	11.64

[a] ΔSCF value.
[b] Empirical energy correction (see Section 4.7).

Table 8
Calculated (6-311G(d,p)) ionization energies for **6b** (all values in eV).

Exp.	MO type	$-\varepsilon_i^{KS}$	TD-DFT	OVGF	"Corrected" $x = 2.32$[b]
8.8	$n_O^\pi - n_N^\pi$	6.48	8.71[a]	9.26	8.80
9.45	$n_{Ge} - n_O^\sigma$	7.19	9.38	9.27	9.51
10.5	$n_O^\pi - n_N^\pi$	7.92	10.35	10.78	10.24
	$n_O^\sigma - \sigma_{Ge-O}$	8.36	10.69	11.22	10.68
	$\sigma_{Ge-O} - \sigma_{Ge-N}$	10.36	12.79	13.14	12.68

[a] ΔSCF value.
[b] Empirical energy correction (see Section 4.7).

were found to be consistent with sp³-hybridization (*vide supra*), the corresponding values for **5b** and **6b** are closer to the 360° value that is expected for sp² hybridization. On the other hand, the XGeY bond angles are reduced significantly in the germylene structures compared to the corresponding precursors, with the largest changes (6–7°) occurring in the aza-compounds **5b** and **6b**. The ring twist angles are also smaller than in the precursors, with the aza–oxa derivative again possessing the smallest value in the series.

IEs were calculated for each species and are listed in Tables 6–8 along with their assignments. The first IE in **4b**, corresponding to the antibonding combination of the heteroatom π lone pair orbitals ($n_S^\pi - n_O^\pi$), is predicted to arise at 9.06 eV by both the ΔSCF (TD-DFT) and OVGF methods. This corresponds well with the enhanced ionization observed at 9.3 eV in the experimental spectrum of the thermolysate from **4a** (Fig. 4). More serious deviations from experiment occur in the OVGF values for the 2nd IE, associated with an MO consisting mainly of the germanium lone pair, and the nearly isoenergetic 3rd and 4th IEs, which are associated with MOs comprised of the bonding combination of the heteroatom π lone pair orbitals and the antibonding combination of the heteroatom σ lone pair orbitals, respectively. Ionizations from these three MOs are predicted to occur at 9.32 and ~10.5 eV by TD-DFT, and at 9.14 and ~11.2 eV by OVGF; the 5th IE is predicted to occur at ~11.5 eV by both methods. All in all, the TD-DFT method agrees more satisfactorily with the experimental spectrum.

Closer agreement between the two methods is obtained for the aza–thia derivative **5b**, and the predicted IEs correlate well with the bands observed in the PE spectrum of the thermolysate from **5a** (Fig. 5). IE₁ and IE₂ are associated with the antibonding combination of the heteroatom π lone pair orbitals ($n_S^\pi - n_N^\pi$) and the germanium lone pair orbital, respectively, and are predicted to occur at 8.4–8.5 eV and 8.8–8.9 eV, respectively. These are consistent with the enhanced ionizations occurring at 8.4 and 9.3 eV in the experimental spectrum. The third ionization band, due to ionization from an MO consisting of the bonding combination of the heteroatom lone pair orbitals, is predicted to occur at 9.7–9.8 eV, in good agreement with the feature occurring at 9.9 eV in the experimental spectrum. The two higher-lying bands, due to ionization from the Ge σ-type skeletal MOs, are predicted to arise in the experimental spectrum at 10.8 and 11.6–11.9 eV, and can thus be

assigned to the bands at 10.5 and 11.65 eV in the experimental spectrum.

The calculated first ionization energy in **6b**, which is associated with the antibonding combination of the heteroatom π lone pair orbitals ($n_N^\pi - n_O^\pi$), varies substantially between the two methods (ΔSCF: 8.71 eV, OVGF: 9.26 eV). Closer agreement is obtained between the calculated values of the second IE, although TD-DFT predicts it to lie *ca.* 0.7 eV above IE₁, while OVGF predicts it to be essentially isoenergetic with IE₁. The experimental spectrum for this compound shows a first ionization band centered at 8.8 eV, in good agreement with the lowest IE calculated by the TD-DFT method. The second ionization energy at 9.45 eV corresponds to the ejection of an electron from the orbital localized mainly on the germanium lone pair, while the third band at 10.5 eV is associated with the bonding combination of the heteroatom π lone pairs orbitals ($n_O^\pi + n_N^\pi$) and the oxygen σ lone pair orbital interacting with the Ge–O bond ($n_O^\sigma - \sigma_{Ge-O}$).

In all three cases, lowest IEs have been located in the experimental spectra that correlate quite well with the values predicted for **4b–6b** by the TD-DFT method. This justifies calculation of the so-called "corrected" values for the higher-lying ionization bands from the Kohn–Sham orbital energies, the results of which are included in Tables 6–8. In all cases, the values obtained agree quite well with the TD-DFT values for the molecules, but it seems that the OVGF method overestimates the electronic correlation. The results of these calculations allow assignment of the lowest IEs in the three germylenes to the ejection of an electron from the antibonding combination of the heteroatom π lone pairs [**4b**: 9.3 eV ($n_S^\pi - n_O^\pi$); **5b**: 8.4 eV ($n_S^\pi - n_N^\pi$); **6b**: 8.8 eV ($n_O^\pi - n_N^\pi$)]. The second bands are associated with the orbital localized mainly on the germanium lone pair, which have been located at 9.4 eV ($n_{Ge} - n_S^\sigma$) in the case of **4b**, 9.3 eV ($n_{Ge} - n_S^\sigma$) in the case of **5b** and 9.45 eV ($n_{Ge} - n_S^\sigma$) for **6b**. Finally, the third IEs, which are associated with the bonding combination of the heteroatom π lone pairs and the unoccupied 4pπ orbital of germanium, are found at 10.7 eV in the spectrum of **4b**, 9.9 eV in that of **5b** and at 10.5 eV in **6b**. It is this molecular orbital that leads to stabilization of these species by delocalisation of the O, N or S π-lone pair electrons into the unoccupied 4p-orbital of germanium (Scheme 1).

Natural Bond Orbital analysis [28] has been applied in order to obtain more precise information about the electronic structures of **4b–6b** and the symmetrically substituted analogues of these molecules (**1b**, **2b**, **3b**), which were studied previously [12,20]. The highest 4pπ orbital electron occupation at germanium occurs in the dithia- (**3b**) and diaza- (**1b**) derivatives (0.34e and 0.33e, respectively), while the lowest value is obtained for the dioxa-compound **2b** (0.25e). Intermediate values are obtained for the mixed derivatives (0.29e for **4b**, 0.34e for **5b** and 0.30e for **6b**). Thus, the greatest degree of π-donation is provided by sulfur and nitrogen, and hence a lower degree of electrophilicity is expected for these derivatives.

The IE associated with ionization of the germanium lone pair electrons (IE$_{nGe}$) is of higher energy in **4b** (IE$_{nGe}$ = 9.4 eV) and **6b** (IE$_{nGe}$ = 9.45 eV) than in **5b** (IE$_{nGe}$ = 9.3 eV). These can be compared to the corresponding IEs in the symmetrically substituted
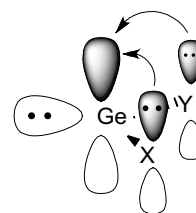
Scheme 1.

derivatives **2b** (IE_{nGe} = 10.0 eV) and **3b** (IE_{nGe} = 9.3 eV) [20]. The corresponding value for **1b** (IE_{nGe} = 8.5 eV) [12] cannot be used in the comparison because of the perturbing influence of the ethyl groups, so a value for the dihydro-substituted analogue (**1b′**; IE_{nGe} = 9.0 eV) has been estimated by TD-DFT (B3LYP/6-311G(d,p)) calculations. The resulting trend in IE_{nGe} (**1b′** < **3b** ∼ **5b** < **4b** < **6b** < **2b**), which predicts **1b′** to be the most nucleophilic germylene in the series, clearly does not follow the trend expected based simply on the total electronegativities of the substituent atoms, as was pointed out earlier for the symmetrically substituted derivatives [20]. Rather, the trend in IE_{nGe} follows the variation in s-character possessed by the germanium lone pair, which is lowered by N-substitution. Taken together with the results of the NBO analysis and experimental IE-values, there is a clear indication that increasing nucleophilicity is accompanied by decreasing electrophilicity. The strong σ-withdrawing effect of oxygen atom and the strong π-donation of nitrogen and sulfur atoms should be considered as the two main factors responsible for the electronic structure of corresponding germylenes, and thus for the energetic position of its lone pair.

3. Summary and conclusions

The FVT/UV-PES technique has allowed the synthesis of germylenes **4b**, **5b** and **6b** by thermal cheletropic elimination from the corresponding 3,4-dimethyl-1-germacyclopent-3-enes **4a–6a**, and measurement of the photoelectron spectra of both sets of molecules. Quite good agreement between theoretical and experimental ionization energy data for the germylenes is observed. Interestingly, the OVGF method provides the best degree of agreement with experiment in the case of the precursors, but is inferior to the TD-DFT method in the case of the germylenes. This underlines the general advisability of using more than a single theoretical method for the interpretation of experimental photoelectron spectra [29].

The first IE of the sulfur-substituted germacyclopentenes **4a** and **5a** is assigned to the MO consisting of a combination of the sulfur π lone pair orbital and the antibonding combination of the σ_{Ge-C}^{-} bonds on the spirocyclic germacyclopentene ring, whereas for **6a** it corresponds to the analogous MO constructed from the nitrogen π lone pair orbital. The next IE is associated with the $\pi_{C=C}$ MO in all three molecules, while the third is associated with the antibonding combination of the σ_{Ge-C}^{-} bonds and the π lone pair orbital on the second heteroatom (O in the cases of **4a**, **6a** and N in the case of **5a**). Finally, there exists a global lowering of the entire set of IEs throughout the series **1** > **3** > **2** in both the germylenes and their precursors.

For the α,α′-heterosubstituted germylenes **4b**, **5b** and **6b** the first PE band is associated with the MO corresponding to the antibonding combination of the π heteroatom lone pairs, while the second IE is associated with the antibonding combination of the germanium lone pair and the σ sulfur (**4b**, **5b**) or oxygen (**6b**) lone pair. Finally, the third IE is associated in all three cases to an MO corresponding to the bonding combination of the π heteroatom lone pairs and the 4pπ orbital on germanium, and hence reflects the degree of stabilization afforded by π-electron donation. The nucleophilic character of these species can be linked directly to the value of the second IE, indicating that the most pronounced nucleophilicity is possessed by the two nitrogen-containing germylenes, in which the degree of π-donation to germanium is highest. Better stabilization of the germanium lone pair in α,α′-heteroatom-substituted cyclic germanediyls can be seen as a compromise between the σ-acceptor and π-donor power of oxygen, nitrogen and sulfur substituents.

4. Experimental

4.1. General procedures

All reactions and handling have been carried out in an inert atmosphere with the use of standard Schlenk and high vacuum line techniques; these compounds are very sensitive to air and moisture. Solvents and intermediate compounds were distilled prior to use. GeCl₂-dioxane [30], and 1,1-dichloro-3,4-dimethylgermacyclopent-3-ene [23] were prepared according to the previously reported methods.

^{1}H NMR spectra were recorded at 400 MHz on a Bruker AMX 400 spectrometer, while ^{13}C NMR spectra were recorded at 125 MHz on a Bruker AM Avance DRX500 spectrometer; chemical shifts are reported in ppm (δ) relative to tetramethylsilane.

4.2. Synthesis of 1,1-diethylamino-1-germa-3,4-dimethylcyclopent-3-ene (**7**) [24]

See Supplementary material.

4.3. Synthesis of α,α′-disubstituted-1-germa-3,4-dimethylcyclopent-3-enes **4a**, **5a** and **6a** **4a**

A solution of 2-hydroxyethanethiol (0.52 g, 6.69 mmol) in 50 mL of tetrahydrofuran was added slowly to a solution of **7** (2.00 g, 6.69 mmol) in 80 mL of tetrahydrofuran. The reaction mixture was refluxed for 1 h. After removal of volatiles under reduced pressure the oily residue was sublimed to afford 1.54 g of **4a** as a colorless solid (m.p. was not determined): ^{1}H NMR (CDCl₃): δ = 1.75 (s, 6H, CH₃), 1.86 and 1.92 (AB-spin system J_{AB} = 8.5 Hz, 4H, GeCH₂), 2.94 (t, J_{HH} = 5.6 Hz, 2H, SCH₂), 3.94 (t, J_{HH} = 5.6 Hz, 2H, OCH₂). ^{13}C{^{1}H} NMR (CDCl₃): δ = 18.8s, GeCH₂), 28.0 (s, CH₃), 34.6 (s, SCH₂), 68.0 (s, OCH₂), 129.8 (S, C=C). MS/EI: calc. for ^{74}GeC₈H₁₄OS: 233.0915; ^{72}GeC₈H₁₄OS: 230.0907; found: m/z = 234 (16, ^{76}Ge M⁺), 232 (66, ^{74}Ge M⁺), 230 (48, ^{72}Ge M⁺), 228 (36, ^{70}Ge M⁺), 152 (13, ^{76}Ge M⁺−DMB), 150 (30, ^{74}Ge M⁺−DMB), 148 (28, ^{72}Ge M⁺−DMB)), 146 (18, ^{70}Ge M⁺−DMB). **5a**: Reaction of 2-aminoethanethiol (0.52 g, 6.69 mmol) and **7** (2.00 g, 6.69 mmol) under similar conditions to those described for **4a** afforded 1.1 g of a colorless liquid after short-path distillation of the crude reaction mixture. From spectroscopic evidence the distillate consists of a mixture of compounds, containing ca. 40% of **5a**. The following signals are tentatively assigned to **5a**: ^{1}H NMR (CDCl₃): δ = 1.87 (s, 6H, CH₃), 2.02 (br s, 4H, GeCH₂), 2.79 (t, J_{HH} = 5.5 Hz, 2H, NCH₂) 2.82 (t, J_{HH} = 5.5 Hz, 2H, SCH₂); the NH-proton could not be assigned unambiguously. MS/EI: calc. for ^{74}GeC₈H₁₅NS: 232.1066; ^{72}GeC₈H₁₅NS: 229.1058; found: m/z = 231 (56, ^{74}Ge M⁺), 229 (41, ^{72}Ge M⁺), 227 (30, ^{70}Ge M⁺), 149 (100, ^{74}Ge M⁺−DMB), 147 (89, ^{72}Ge M⁺−DMB), 145 (55, ^{70}Ge M⁺−DMB). **6a**: From 2-aminoethanol (0.37 g, 5.99 mmol) and 7 (1.79 g, 5.99 mmol), 0.66 g (51%) of product **6a** were obtained as a colorless liquid after short-path distillation. ^{1}H NMR (CDCl₃): δ = 1.67 (br s, 4H, GeCH₂), 1.71 (s, 6H, CH₃), 2.78 (t, J_{HH} = 5.3 Hz, 2H, NCH₂), 3.72 (t, J_{HH} = 5.3 Hz, 2H, OCH₂). ^{13}C NMR (CDCl₃): δ = 19.1 (s, GeCH₂), 22.6 (s, CH₃−C=), 44.6 (s, NCH₂), 67.2 (s, OCH₂), 129.3 (s, C=C). MS/EI: calc. for ^{74}GeC₈H₁₅NO: 216.046; ^{72}GeC₈H₁₅NO: 213.0452; found: m/z = 215 (28, ^{74}Ge M⁺), 213 (20, ^{72}Ge M⁺), 211 (16, ^{70}Ge M⁺).

4.4. UV photoelectron spectroscopy

The photoelectron spectra were recorded on a custom-built, three-part spectrometer equipped with a main body device

(Meca2000), He–I radiation source (Focus) and a spherical analyser (Omicron). The spectrometer functions at a constant analyser energy and is monitored by a microcomputer supplemented with a digital-analogue converter. The spectra result from single scans consisting of 2048 data points and are accurate to within 0.05 eV. They are calibrated against the autoionization of xenon at 12.13 and 13.45 eV, and nitrogen at 15.59 eV and 16.98 eV. Sample manipulations were carried out in a thermolysis oven attached directly to the inlet probe; the distance between the oven exit and the ionization head does not exceed 1 cm. Precursors **4a–6a** were slowly vaporized under low pressure (10^{-7} torr in the ionization chamber) directly in the oven, with continuous analysis of the gaseous thermolysate.

4.5. Direct injection mass spectrometric analysis

Mass spectral fragmentation data were recorded using a Hewlett Packard 5975a mass spectrometer (operating in electron impact mode at 70 eV) by direct injection of compounds into the ionization beam. Sample introduction was done from an inlet probe under argon atmosphere, where it was degassed and then distilled slowly under high vacuum (10^{-5} mbar). Once the characteristic mass spectrum of the precursor appeared, the passing vapor was rapidly heated (microresistance associated with an electronic controller, $80^\circ \, s^{-1}$) and a series of spectra of the thermolysis products was obtained.

4.6. Dimethyldisulfide trapping experiments

A solution of precursor **4a**, **5a** or **6a** (0.8 mmol) in a large excess of neat dimethyldisulfide (5 mL) was sealed in a Pyrex tube under vacuum, and the contents were heated at 120 °C for 12 h. The reaction mixtures were then analysed by MS. The reaction mixtures each exhibited mass spectral fragmentation patterns consistent with the formation of the corresponding germylene trapping product (**4c–6c**) along with small amounts of (tetramethylthio)germane [25]. **4c**: calc. for $^{74}GeC_4H_{10}OS_3$: 243.9106; found: $m/z = 244$ ($M^{\cdot+}$, 39), 196 ($M-SCH_3$, 100), 150 ($M-(SCH_3)_2$, 91); **5c**: calc. for $^{74}GeC_4H_{11}NS_3$: 242.9265; found: $m/z = 243$ ($M^{\cdot+}$), 196 ($M-SCH_3$); 6c: calc. for $^{74}GeC_4H_{11}NOS_2$: 226.9494; found: $m/z = 227$ (M^+), 133 ($M-2^*SCH_3$).

4.7. Computational details

Calculations were performed using the GAUSSIAN 98 [31] program package using the density functional theory [32] method. Geometry optimizations were carried out at the B3LYP [33]/6-311G(d,p) level of theory, and were followed by frequency calculations in order to verify that the stationary points obtained were true energy minima.

To calculate the first ionic states, time dependent density functional theory (TD-DFT) [34] was used. This calculation is based on the evaluation of the electronic spectrum of the low lying ion, described by the ΔSCF corresponding to the first vertical ionization energy IE_1v^{cal}, calculated as the difference $E_{cation} - E_{neutral \, molecule}$. The vertical IEs were also calculated at the *ab initio* level employing the outer valence green's function (OVGF) method [35], which includes electron correlation and electron relaxation effects. So-called "corrected" IEs were calculated by applying a uniform shift of $x = -IE_v^{exp} - \varepsilon^{KS}(HOMO)$, where $\varepsilon^{KS}(HOMO)$ is the highest occupied B3LYP/3-111G(d,g) Kohn–Sham MO energy of the ground state molecule and IE_v^{exp} is the lowest experimental ionization energy of the molecule, as suggested previously by Stowasser and Hoffman [36] and in our recent study of different methods for the calculation of ionization energies [22].

Appendix A. Supplementary material

Cartesian coordinates for the calculated structures **4a**, **5a**, **6a** and **4b**, **5b**, **6b**. Supplementary data associated with this article can be found, in the online version, at doi:10.1016/j.jorganchem.2008.09.069.

References

[1] (a) For recent reviews of simple systems, see: P.P. Gaspar, R. West, in: Z. Rappoport, Y. Apeloig (Eds.), The Chemistry of Organic Silicon Compounds, vol. 2, John Wiley and Sons Ltd., Chichester, 1998 (Chapter 43);
(b) S.E. Boganov, M.P. Egorov, V.I. Faustov, O.M. Nefedov, Z. Rappoport (Eds.), The Chemistry of Organic Germanium, Tin and Lead Compounds, John Wiley and Sons, Chichester, 2002 (Chapter 1);
(c) W.P. Neumann, Chem. Rev. 91 (1991) 311.
[2] (a) For recent reviews of stable heterosubstituted silylenes and germylenes, see: M. Driess, H. Grützmacher, Angew. Chem., Int. Ed. Engl. 35 (1996) 828;
(b) R. West, M. Denk, Pure Appl. Chem. 68 (1996) 785;
(c) M. Denk, R. West, R. Hayashi, Y. Apeloig, R. Pauncz, M. Karni, N. Auner, J. Weis (Eds.), Organosilicon Chemistry II – From Molecules to Materials, VCH, Weinheim, 1996, p. 251;
(d) J. Barrau, G. Rima, Coord. Chem. Rev. 178–180 (1998) 593;
(e) N. Tokitoh, R. Okazaki, Coord. Chem. Rev. 210 (2000) 251.
[3] D.H. Harris, M.F. Lappert, J. Chem. Soc., Chem. Commun. (1974) 895.
[4] D.H. Harris, M.F. Lappert, J.B. Pedley, G.J. Sharp, J. Chem. Soc., Dalton Trans. (1976) 945.
[5] W.A. Herrmann, M. Denk, J. Behm, W. Scherer, F.R. Klingan, H. Bock, B. Solouki, M. Wagner, Angew. Chem., Int. Ed. Engl. 31 (1992) 1485.
[6] (a) A.J. Arduengo III., R.L. Harlow, M. Kline, J. Am. Chem. Soc. 113 (1991) 361;
(b) A.J. Arduengo III., H.V. Rasika Dias, R.L. Harlow, M. Kline, J. Am. Chem. Soc. 114 (1992) 5530;
(c) A.J. Arduengo III., J.R. Goerlich, W.J. Marshall, J. Am. Chem. Soc. 117 (1995) 11027.
[7] M. Denk, R. Lennon, R. Hayashi, R. West, A.V. Belyakov, H.P. Verne, A. Haaland, M. Wagner, N. Metzler, J. Am. Chem. Soc. 116 (1994) 2691.
[8] (a) A.J. Arduengo III., H. Bock, H. Chen, M. Denk, D.A. Dixon, J.C. Green, W.A. Herrmann, N.L. Jones, M. Wagner, R. West, J. Am. Chem. Soc. 116 (1994) 6641;
(b) M. Denk, J.C. Green, N. Metzler, M. Wagner, J. Chem. Soc., Dalton Trans. (1994) 2405.
[9] (a) S.G. Urquhart, A.P. Hitchcock, J.F. Lehmann, M.K. Denk, Organometallics 17 (1998) 2352;
(b) J.F. Lehmann, S.G. Urquhart, L.E. Ennis, A.P. Hitchcock, K. Hatano, S. Gupta, M.K. Denk, Organometallics 18 (1999) 1862.
[10] C. Boehme, G. Frenking, J. Am. Chem. Soc. 118 (1996) 2039.
[11] C. Heinemann, W.A. Hermann, W. Thiel, J. Organomet. Chem. 475 (1994) 73.
[12] A. Laporte-Chrostowska, S. Foucat, T. Pigot, V. Lemierre, G. Pfister-Guillouzo, Main Group Met. Chem. 1 (2002) 55.
[13] P. Rivière, M. Rivière-Baudet, J. Satgé, in: G. Wilkinson (Ed.), Comprehensive Organometallic Chemistry, Pergamon Press, Oxford, 1982, p. 402 (Chapter 10).
[14] B. Cetinkaya, I. Gümrükçu, M.F. Lappert, J.L. Atwood, R.D. Rogers, M.J. Zaworotko, J. Am. Chem. Soc. 102 (1980) 2088.
[15] A. Meller, C.-P. Gräbe, Chem. Ber. 118 (1985) 2020.
[16] (a) J. Barrau, G. Rima, T. El Amraoui, Inorg. Chem. Acta 241 (1996) 9;
(b) J. Barrau, G. Rima, T. El Amraoui, Organometallics 17 (1998) 607.
[17] N.N. Zemlyansky, I.V. Borisova, M.G. Kuznetsova, V.N. Krustalev, Y.A. Ustynyuk, M.S. Nechaev, V.V. Lunin, J. Barrau, G. Rima, Organometallics 22 (2003) 1675.
[18] P. Jutzi, W. Steiner, Chem. Ber. 109 (1976) 1575.
[19] (a) H. Lavayssière, G. Dousse, J. Satgé, Recl. Trav. Chim. Pays-Bas 107 (1988) 440;
(b) H. Lavayssière, G. Dousse, J. Satgé, Phos. Sulf. Sil. Rel. Elem. 53 (1990) 411;
(c) S. Mazières, H. Lavayssière, Inorg. Chim. Acta 252 (1996) 25;
(d) C. Laurent, S. Mazières, H. Lavayssière, P. Mazerolles, G.J. Dousse, Organomet. Chem. 452 (1993) 41.
[20] T. Pigot, S. Foucat, G. Pfister-Guillouzo, J. Mol. Struct. 782 (2006) 36.
[21] P. Rivière, M. Rivière-Baudet, J. Satge, A.G. Davies, in: E.W. Abel, F.G.A. Stone, G. Wilkinson (Eds.), Comprehensive Organometallic Chemistry II, vol. 1, Pergamon, New York, 1995, pp. 137–216.
[22] V. Lemierre, A. Chrostowska, A. Dargelos, H. Chermette, J. Phys. Chem. A 109 (2005) 8348.
[23] V. Lemierre, A. Chrostowska, A. Dargelos, P. Baylère, W.J. Leigh, C.R. Harrington, Appl. Organomet. Chem. 18 (2004) 676.
[24] J. Satgé, G. Dousse, J. Organomet. Chem. 61 (1973) C26–C32.
[25] K.A. Hooton, A.L. Allred, Inorg. Chem. 4 (1965) 671.

[26] K.M. Mackay, in: S. Patai (Ed.), The Chemistry of Organic Germanium, Tin and Lead Compounds, John Wiley and Sons, Chichester, 1995, p. 97 (Chapter 2).

[27] K. Kimura, S. Katsumata, Y. Achiba, T. Yamazaki, S. Iwata, Handbook of HeI Photoelectron Spectra of Fundamental Organic Molecules, Halsted Press, New York, 1981.

[28] (a) A.E. Reed, L.A. Curtiss, F. Weinhold, Chem. Rev. 88 (1988) 899;
(b) J.P. Foster, F. Weinhold, J. Am. Chem. Soc. 102 (1980) 7211.

[29] (a) S. Joantéguy, G. Pfister-Guillouzo, H. Chermette, J. Phys. Chem. 103 (1999) 3505;
(b) A. Chrostowska, K. Miqueu, G. Pfister-Guillouzo, E. Briard, J. Levillain, J.-L. Ripoll, J. Mol. Spectrosc. 205 (2001) 323;
(c) R. Bartnik, P. Baylère, A. Chrostowska, A. Galindo, S. Lesniak, G. Pfister-Guillouzo, Eur. J. Org. Chem. (2003) 2475.

[30] S.P. Kolesnikov, A.I. Ioffe, O.M. Nefedov, Izv. Akad. Nauk SSSR, Ser. Khim. (1975) 978.

[31] GAUSSIAN 98: M.J. Frisch, G.W. Trucks, H.B. Schlegel, G.E. Scuseria, M.A. Robb, J.R. Cheeseman, V.G. Zakrzewski, J.A. Montgomery, R.E. Stratman, J.C. Burant, S. Dapprich, J.M. Millam, A.D. Daniels, K.N. Kudin, M.C. Strain, O. Farkas, J. Tomasi, V. Barone, M. Cossi, R. Cammi, B. Mennucci, C. Pomelli, C. Adamo, S. Clifford, J. Ochterski, G.A. Petersson, P.Y. Ayala, Q. Cui, K. Morokuma, D.K. Malick, A.D. Rabuck, K. Raghavachari, J.B. Foresman, J. Cioslowski, J.V. Ortiz, A.G. Baboul, B.B. Stefanov, G. Liu, A. Liashenko, P. Piskorz, I. Komaromi, R. Gomperts, R. Martin, D.J. Fox, D.T. Keith, M.A. Al-Laham, C.Y. Peng, A. Nanayakkara, C. Gonzalez, M. Challacombe, P.M.W. Gill, B. Jonhson, W. Chen, M.W. Wong, J.L. Andres, M. Head-Gordon, E.S. Replogle, J.A. Pople, GAUSSIAN 98, Revision A.7, GAUSSIAN, Inc., Pittsburgh PA, 1998.

[32] (a) R.G. Parr, W. Yang, Functional Theory of Atoms and Molecules, Oxford University Press, New York, 1989;
(b) M.J. Frish, G.W. Trucks, J.R. Cheeseman, in: J.M. Semminario (Ed.), Recent Development and Applications of Modern Density Functional Theory, Theoretical and Computational Chemistry, vol. 4, Elsevier, Amsterdam, Lausanne, New York, Oxford, Shannon, Tokyo, 1996, pp. 679–707.

[33] (a) A.D. Becke, Phys. Rev. 38 (1988) 3098–3100;
(b) A.D. Becke, J. Chem. Phys. 98 (1993) 5648–5652;
(c) C. Lee, W. Yang, R.G. Parr, Phys. Rev. B37 (1988) 785–789.

[34] (a) R.E. Stratmann, G.E. Scuseria, M.J. Frisch, J. Chem. Phys. 109 (1998) 8218;
(b) M.E. Casida, C. Jamorski, K.C. Casida, D.R. Salahub, J. Chem. Phys. 108 (1998) 4439.

[35] (a) W. Von Niessen, J. Schirmer, L.S. Cederbaum, Comp. Phys. Rep. 1 (1984) 57;
(b) J.V. Ortiz, J. Chem. Phys. 89 (1988) 6348.

[36] R. Stowasser, R. Hoffmann, J. Am. Chem. Soc. 121 (1999) 3414.